

Excited-state production in collisions of H and He with N₂, CO, and O₂ over the energy range 150–2400 eV

G. H. Bearman and J. J. Leventhal

Department of Physics, University of Missouri—St. Louis, St. Louis, Missouri 63121

(Received 20 May 1977)

Spectroscopic analysis of optical emissions resulting from collisions between diatomic molecules (N₂, CO, O₂) and hydrogen or helium atoms has been performed over the kinetic energy range ~150–2400 eV. The data yield product vibronic-state distributions from collision-induced excitation, impact ionization, and excitation transfer processes. For most of the processes observed spin is conserved. It was found that vibrational-state distributions of excited electronic product molecular ions were not in accord with those predicted from a simple vertical transition model. Excited neutral molecules, on the other hand, exhibited state distributions that could be characterized by this model.

I. INTRODUCTION

Within the last few years spectroscopic analysis of collision-produced radiation has provided detailed information on internal-energy-state distributions of product species resulting from low-energy collision processes.¹ Aside from the intrinsic interest in these state distributions, these data can be of considerable value for laboratory simulation of atmospheric and astrophysical processes and also in the design and construction of new laser devices. Most of these studies have involved ion-neutral collision systems because of the relative ease of producing and guiding low-energy ion beams. It is of interest, however, to compare these ion-neutral data to similar data resulting from neutral-neutral collisions. This paper reports the results of our study of collisions between hydrogen atoms or helium atoms with simple diatomic molecules. Most of the data reported here involves N₂ targets; however, data are also presented for CO and O₂ targets. The atomic beams were produced by neutralization of an appropriate ion beam (H⁺ or He⁺), and for this reason the present results are restricted to studies above about 150 eV; the upper limit was 2.4 keV.

An important difference between the ion-neutral and neutral-neutral systems is that in the former charge transfer excitation (CTE) collisions dominate at these energies so that most of the observed emissions are from excited ionic products or neutralized projectile ions. On the other hand, impact ionization in neutral-neutral collisions occurs primarily at higher kinetic energies so that collision-induced excitation (CIE) processes yielding excited atoms or molecules may be studied more readily. It has been shown in a wide variety of systems that CTE processes at low energies, with few exceptions, yield product molecular-ion vibronic-state distributions that differ substan-

tially from those predicted by a simple vertical transition model; as the kinetic energy is increased these distributions tend toward the Franck-Condon (vertical) picture.^{2–4} The present results provide state distributions of neutral product molecules from CIE processes. It is particularly intriguing that our data show that these distributions follow the vertical transition model over the entire energy range. Previous studies of hydrogen atom-diatom molecule collisions at higher energies are consistent with our observations.^{5,6} In fact, earlier work on CIE by ion impact, using energy-loss techniques, have also shown Franck-Condon (FC) distributions of electronically excited neutral product molecules.^{7,8} One earlier study of H⁺-NO(X) CIE from our laboratory,⁹ using spectroscopic techniques, showed vertical vibrational state populations of NO(A). The evidence now suggests that vertical excitation for neutral excitation may be more general than had previously been thought.

II. EXPERIMENTAL

The data reported in this paper were obtained by spectral analysis of collision produced luminescence. A beam of either hydrogen or helium atoms is directed into a collision cell containing the target diatomic gas at 6 mTorr pressure. This pressure is somewhat higher than that used by us in previous ion-molecule experiments¹; however, appropriate experiments in which the target gas pressure was varied over the range 1–6 mTorr showed that at 6 mTorr only single-collision processes were being observed.

The atomic beams were produced by charge-transfer neutralization of a mass-analyzed H⁺ or He⁺ beam; the neutral-beam energy is taken to be that of the ion prior to charge transfer. Un-neutralized ions were electrostatically eliminated be-

tween the neutralization cell and the atom-diatom collision cell. A tantalum grid located behind the collision cell is used to monitor the neutral-beam current by detection of secondary electrons. No attempt was made to calibrate the neutral-beam flux, so absolute cross sections are not reported. Photons resulting from the atom-diatom collisions emerge through a slot in the collision cell and enter a 0.25 m scanning monochromator; detection is accomplished with a cooled photomultiplier (extended S-20 cathode) and single-photon counting. The monochromator entrance slit is oriented parallel to the primary-beam axis. Emission spectra are obtained by stepwise scanning through a given wavelength region and recording the number of photons at each wavelength setting; signal averaging is accomplished by repetitively scanning the wavelength region of interest. In all cases data were accumulated until the error bar ($\pm\sqrt{N}$) associated with the highest count total was less than five percent of this total. Apparatus control and data acquisition are performed by a PDP8/E mini-computer which also corrects for variations in the spectral efficiency.¹ Although the beam was stable for long periods of time (greater than several hours), it was sampled at the end of each counting interval and the signal normalized to account for any beam variations.

The H-atom beam was obtained by charge transfer of protons with xenon gas. Metastable H($2s$) were easily quenched by the field used to remove unneutralized protons; this same field would also ionize Rydberg H atoms with $n \geq 22$. Additionally, cross sections for production of H($n = 13-28$) are very small at these energies¹⁰ so that it is concluded that the hydrogen-atom beam used in these studies was free of excited states. Further support for this conclusion comes from the absence of Balmer emissions from an unscattered beam.

The He beam was produced by He⁺-He charge transfer; however, in this case there is a metastable component of the beam. It is difficult to determine the exact internal-energy-state population of the He beam, but limits on the metastable component can be set. Direct electron capture into the ground state or metastable states cannot be detected by us. We can, however, detect radiative cascade from higher electronic states into the metastable He(2^1S) and He(2^3S) states by observing the luminescence spectrum from He⁺-He collisions. Figure 1 is a partial Grotrian diagram for He I showing the lines observed from 1-keV He⁺-He collisions; this experiment was performed with target He gas in the collision cell in front of the optical system. The sum of the emission cross sections for lines feeding the metastable states then yields a lower limit on the metastable frac-

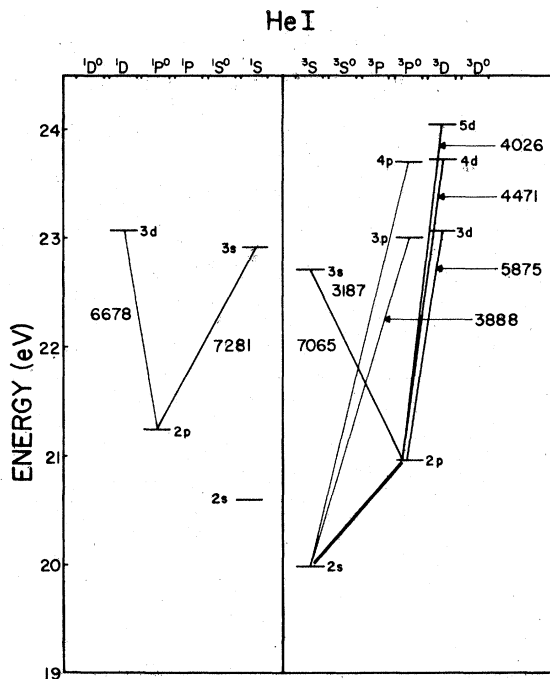


FIG. 1. Partial term diagram of He I. The transitions shown are those observed in 1-keV He⁺-He collisions. The heavy line represents the strong 1083-nm transition which cannot be observed in these experiments, but feeds the metastable 2^3S state.

tion of the beam. Note that for ion-neutral collisions absolute cross sections can be obtained. A typical result is that at least 1%-2% of the neutral He beam is in the 2^3S metastable state. Because $2^1P^0 \rightarrow 1^1S$ is greatly favored over $2^1P^0 \rightarrow 2^1S$, this latter metastable state is only formed directly.

In addition to the He⁺-He experiment described above, one additional experiment designed to yield information on the relative populations of He(2^1S) and He(2^3S) was performed. The He-Ne laser is known to be pumped by excitation transfer from He(2^1S) to the upper level of the 632.8 nm transition. Although this process occurs at thermal energies in a laser tube, it was nevertheless felt that this resonant excitation transfer process should produce relatively high yields of 632.8 nm radiation in our experiment if the 2^1S state was present to any appreciable degree. Low-count rates at 632.8 nm were observed. In fact, several other Ne I lines, with upper states more nearly in resonance with the 2^3S state, were observed with substantial intensity. This He-Ne experiment thus supports the contention that the major metastable component of the helium-atom beam is He(2^3S).

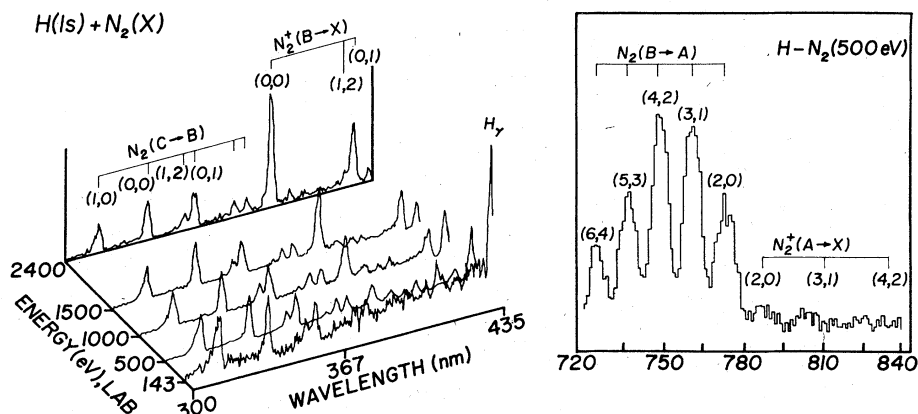


FIG. 2. Emission spectra from $H(1s) + N_2(X)$ collisions at various laboratory kinetic energies corrected for relative spectral efficiency. The prominent $N_2(B \rightarrow A)$ emissions are shown in the inset. Band heads of several systems are indicated (Ref. 11) including some of the (unobserved) Meinel system $N_2^+(A \rightarrow X)$. The resolution was 2 nm full width at half maximum (FWHM).

III. RESULTS

Spectra from $H-N_2$ collisions at various kinetic energies are presented in Fig. 2. N_2 emissions from the $C^3\Pi_u \rightarrow B^3\Pi_g$ second-positive (2P) and $B^3\Pi_g \rightarrow A^3\Sigma_u^+$ first-positive (1P) systems are observed over the entire range of kinetic energies. The intensity of the 1P emissions relative to the 2P emissions indicates that $N_2(B)$ is produced directly as well as by cascading, although other (unobservable) cascades¹¹ to $N_2(B)$, such as $D \rightarrow B$ fourth positive, $W \rightarrow B$, and $B' \rightarrow B$, may also populate $N_2(B)$. As the kinetic energy is increased, emissions from the $N_2^+(B^2\Sigma_u^+ \rightarrow X^2\Sigma_g^+)$ first-negative (1N) band system become stronger. At 2.4 keV, the highest energy for which we have data, the $N_2^+(1N)$ emissions, produced by impact ionization, are comparable in intensity to those from $N_2(2P)$; according to Birely,⁶ the total cross section for production of $N_2^+(B)$ overtakes that for production of $N_2(C)$ at ~ 7 keV in $H-N_2$ collisions. CIE of the neutral H atom also occurs as evidenced by the observation of Balmer emissions; the apparent decrease in the $H\gamma$ intensity with increasing kinetic energy is a kinematic effect. At the higher projectile energies the strength of the Balmer emissions appears to decrease because a large fraction of the fast excited H atoms move out of the field of view of the optical detection system before radiating.¹²

Data for $He-N_2$ collisions are presented in Fig. 3. The most prominent features are from the $N_2^+(1N)$ band system, and are likely due to $He(2^3S)-N_2$ Penning ionization processes at the lower energies; some CIE is observed at all kinetic energies. No $N_2^+(A^2\Pi_u \rightarrow X^2\Sigma_g^+)$ Meinel emissions were detected for either H- or He-atom impact over the

entire range of kinetic energies.

Data were also obtained for O_2 and CO targets. Figure 4 shows a 1-keV He-CO spectrum, and Fig. 5 a 2-keV H-CO spectrum. Both projectiles produce substantial amounts of $CO^+(A^2\Pi_u)$ as indicated by the observation of $CO^+(A \rightarrow X)$ Comet tail emissions; $CO^+(B \rightarrow X)$ first-negative emissions were weak relative to the Comet tail bands. In calculating the relative populations of $CO^+(A)$ and $CO^+(B)$ from the data, account must be taken of the different lifetimes of the two radiating states, the path length over which emissions are detected, and the approximate speed of the radiating specie. (This is the same kinematic effect noted above in connection with the observed decrease of Balmer emission intensity with increasing kinetic energy.) Since the $CO^+(A)$ lifetime ($\sim 3 \mu\text{sec}$) is much longer¹³ than that of $CO^+(B)$

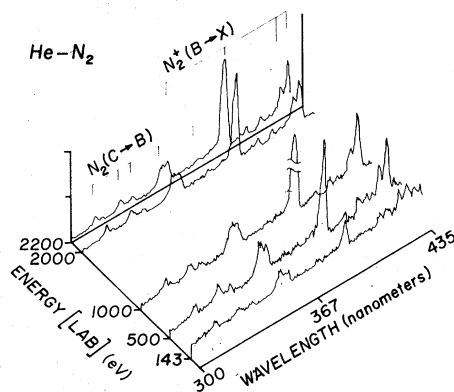


FIG. 3. $He-N_2(X)$ spectra at various kinetic energies, corrected for spectral efficiency. See Fig. 2 for the indicated band heads of $N_2(C \rightarrow B)$ and $N_2^+(B \rightarrow X)$. The resolution was 2 nm FWHM.

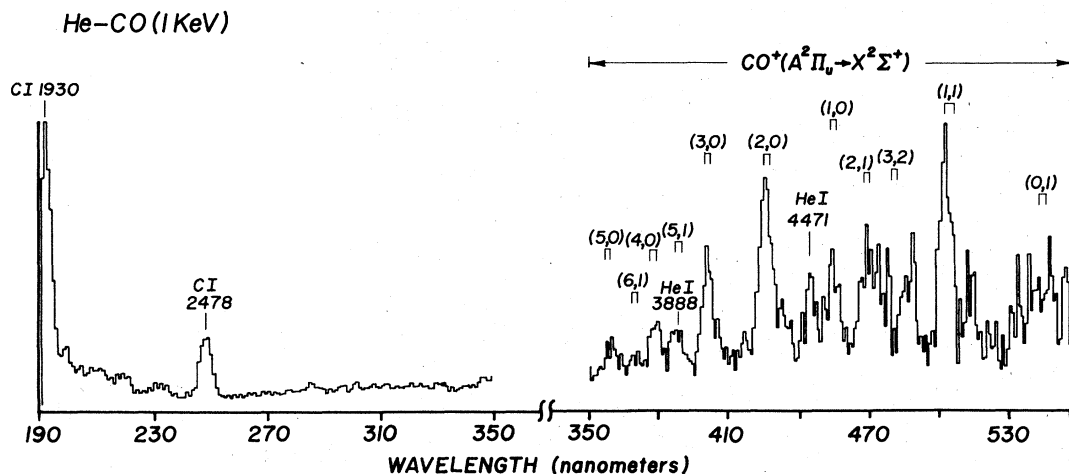


FIG. 4. Emission spectrum from 1-keV (lab) He-CO collisions, corrected for spectral efficiency. The CI line at 1930 is exaggerated by the low spectral efficiency near 190 nm. The break in the wavelength axis is to emphasize that there is no intensity relationship between the two sections. Band heads are from Ref. 11. The resolution was 5 nm FWHM.

(~50 nsec), the correction is important even at low energies. For example, if only 10 eV kinetic energy is transferred to the CO^+ , the lifetime correction, coupled with the data, gives a ratio of $\text{CO}^+(A):\text{CO}^+(B)$ of about 30.

Neutral excitation of CO was detected only for H impact; the $v'=0$ progression of the $\text{CO}(b^3\Sigma^+ - a^3\Pi)$ third-positive (3P) band system was observed. Additional neutral CO emissions were observed at longer wavelengths; $d^3\Delta - a^3\Pi$, $e^3\Sigma^- - a^3\Pi$, and $a^1\Sigma^+ - a^3\Pi$ as indicated in Fig. 6. The combination of low photon flux and overlapping spectral features prevented the determination of specific vibrational-state distributions for neutral CO emissions.

A 1-keV H- O_2 impact-produced spectrum is

shown in Fig. 7. The spectral features are from the $\text{O}_2^+(b - a)$ first-negative-band system. In this case, individual band heads are too close to permit resolution with our apparatus so that the peaks are sequences of bands. A search of the region 190-400 nm revealed the presence of low yields of $\text{O}_2^+(A - X)$ second-negative emissions, but only at energies above 1 keV. At all energies these emissions were much less intense than the $\text{O}_2^+(1N)$ emissions. Figure 8 is a spectrum resulting from He- O_2 impact and again the dominant features are from the $\text{O}_2^+(1N)$ system. However, by comparing the relative peak heights of the unresolved sequences to those produced by H-atom impact it is clear that the vibrational state distributions for the two cases are substantially different. For

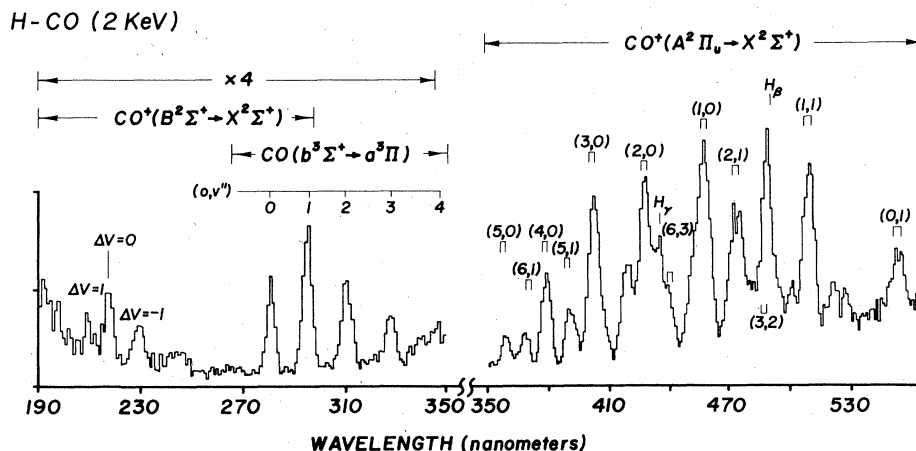


FIG. 5. Emission spectrum from 2-keV (lab) H-CO collisions, corrected for spectral efficiency. The abscissa and resolution are the same as in Fig. 4. Band heads are from Ref. 11.

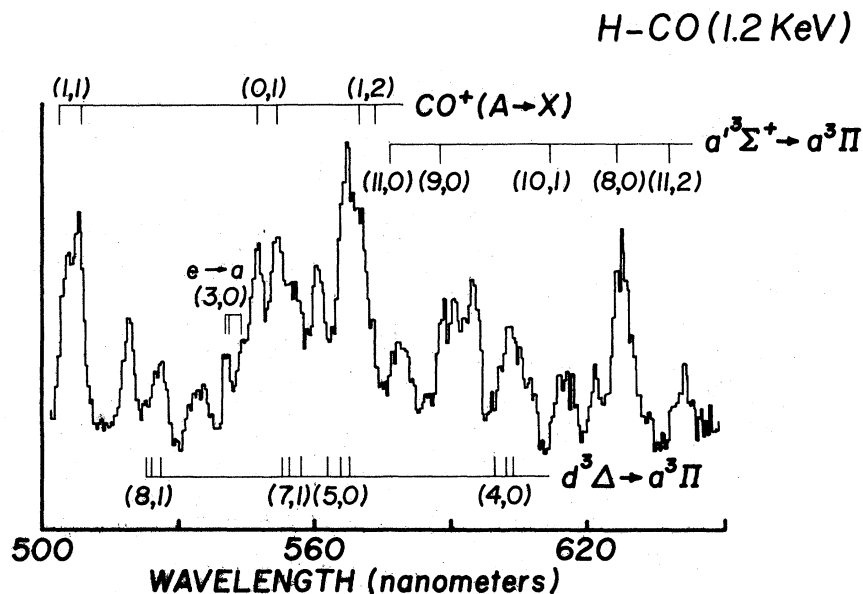


FIG. 6. Spectrum from 1.2-keV (lab) H-CO collisions corrected for spectral efficiency. The indicated band heads (Ref. 11) are for CO emissions except for the $\text{CO}^+(A \rightarrow X)$ band system. The resolution was 2 nm FWHM.

both projectiles the respective distributions changed very little from 200 eV–2.4 keV consistent with Birely's H- O_2 results⁵ at higher energies (up to 25 keV).

In contrast to the H- O_2 results many O I lines were observed from He- O_2 collisions. A few O II lines were also observed, in particular, the 407.5-nm $3d^4F \rightarrow 3p^4P^0$ transition. He impact produced higher yields of $\text{O}_2^+(2N)$ emissions relative to those from $\text{O}_2^+(1N)$ than did H impact. Birely's study also showed that $\text{O}_2^+(b)$ is the dominant radiating O_2^+ state

resulting from H- O_2 collisions at higher energies.⁵ The $\text{O}_2^+(A)$ resulting from He- O_2 collisions is likely due to Penning ionization since $\text{O}_2^+(2N)$ emissions are observed at low energies as shown in Fig. 8.

IV. DISCUSSION

At the lowest kinetic energies studied, the collision-produced emission spectra resulting from H- and He-atom impact differ significantly. This is illustrated in Fig. 9, where the 143-eV H- N_2

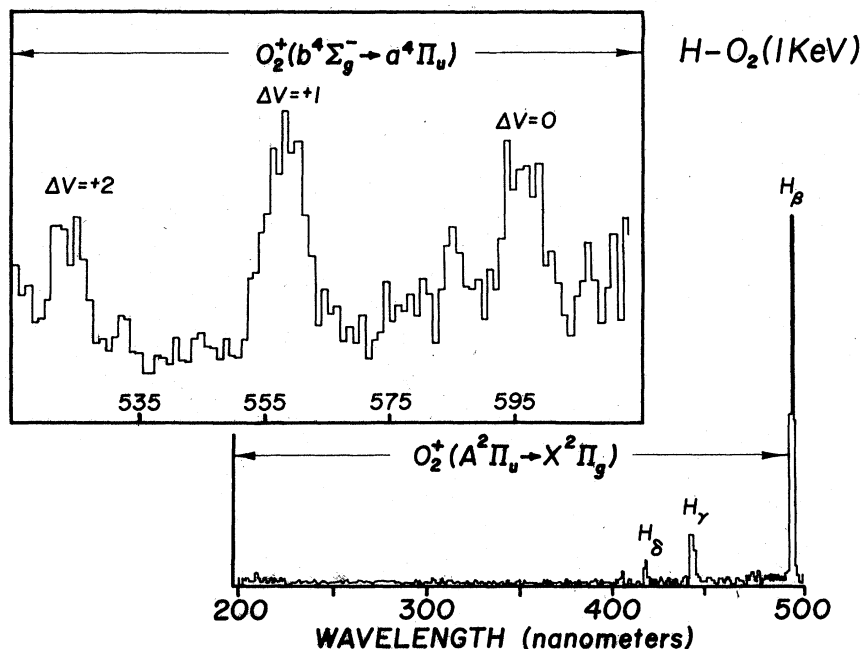


FIG. 7. Emission spectra from 1-keV (lab) H- O_2 collisions which are corrected for spectral efficiency. Note the absence of $\text{O}_2^+(A \rightarrow X)$ emissions. The resolution was 5 nm FWHM.

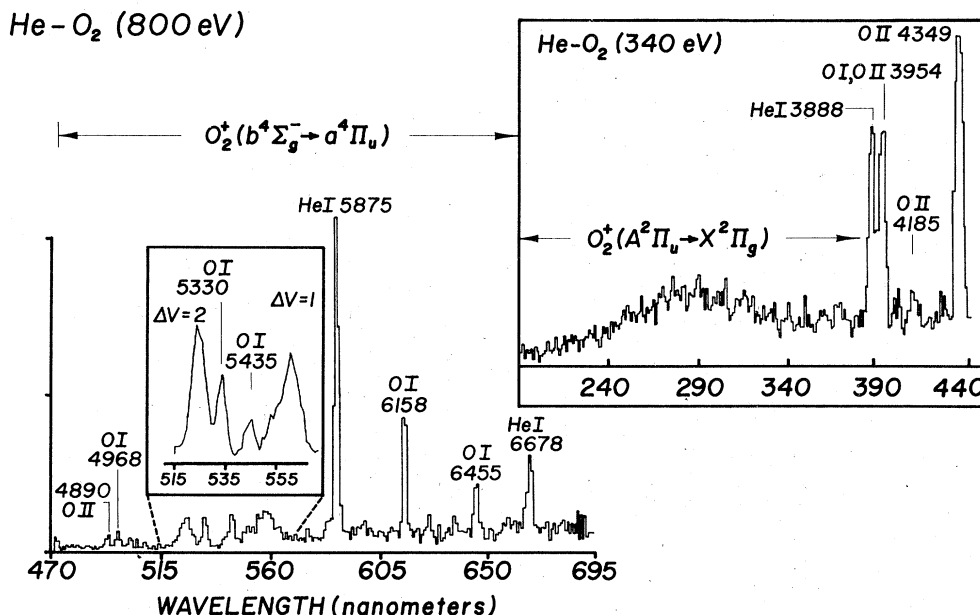


FIG. 8. Spectra from 800-eV (lab) and 340-eV He-O₂ (lab) collisions. O₂⁺(A → X) emissions are more intense than in Fig. 7. The resolution was 5 nm FWHM. All the spectra have been corrected for relative spectral response of the detector.

and He-N₂ results are compared. The radiating species produced by H-atom impact are N₂(C), N₂(B), and excited H atoms, all of which result from CIE processes. He impact, on the other hand, produces preponderantly N₂⁺(B); weaker emissions from N₂(C) are also observed. N₂⁺(B) is probably formed by Penning ionization involving the metastable He(2³S) component of the primary beam; however, it is uncertain whether the N₂(2P) emissions result from CIE involving the ground-state component of the He beam or excitation transfer from the metastable component. Production of N₂(C³Π_u) by He(1¹S)-N₂(X¹Σ_g⁺) CIE would be a violation of the Wigner spin rule,¹⁴ while excitation transfer is not. However, excitation transfer is ~8 eV exothermic and has not been observed in thermal He-N₂ collisions.¹⁵ Thus, it seems unlikely that such collisions are the origin of N₂(2P) emissions in this work. We believe, therefore, that spin forbidden He(1¹S)-N₂ CIE collisions are responsible for the production of N₂(C). It is, however, also possible that CIE in He(triplet)-N₂(singlet) collisions having He(triplet) and N₂(triplet) products could be responsible for the N₂(2P) emissions. It is interesting that while we have not attempted to obtain absolute cross sections, the emission cross sections for the N₂(2P) system are observed to be considerably larger for H-atom impact than He impact. For example, if it is assumed that the detection efficiencies of hydrogen atoms and helium atoms are the same, then the

ratio of the *apparent* cross sections is ~10, in favor of H-atom impact. This higher CIE cross section may thus be understood in terms of the Wigner spin rule since H(doublet) + N₂(singlet) → N₂(triplet) + H(doublet) conserves spin.

From the standpoint of spin conservation during the collisions the results for CO targets are analogous to those obtained with N₂ targets; that is, H-atom impact yields neutral triplet products, while He impact does not (see Figs. 5 and 6). For O₂(X³Σ_g⁻) targets no neutral molecular emissions were observed with either hydrogen-atom or helium impact. The optically active states of O₂ are either triplets or singlets, both of which are spin allowed in excitation transfer collisions with HE(2³S) or CIE with H(1²S); production of singlet states of O₂ in He(1s¹S)-O₂(X³Σ_g⁻) CIE processes is spin forbidden (assuming no accompanying He excitation). Since the O₂ molecule is a weak light emitter,¹⁶ the absence of neutral emissions does not necessarily imply that neutral excitations do not occur.

Aside from Balmer emissions, no atomic lines were observed in H-atom collisions with N₂, CO, and O₂. Numerous OI lines were observed from He-O₂ collisions, but only a few weak CI and NI lines from He-CO and N₂ collisions, respectively. The upper states of the observed OI lines lie ~11–13 eV above the ground state of atomic oxygen, and since the dissociation energy of O₂ is 5.1 eV, 16–18 eV is required to produce these upper states. This amount of energy is available in

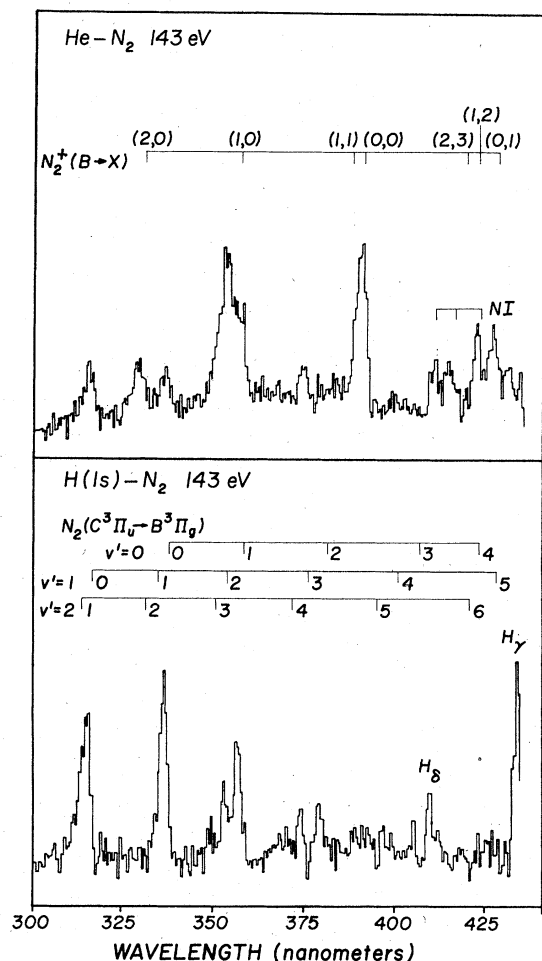


FIG. 9. Emission spectra from 143-eV (lab) H-N₂ collisions corrected for spectral efficiency. Band heads are from Ref. 11. The resolution was 2 nm FWHM.

He(2³S) so that excitation transfer, without conversion of kinetic energy to internal energy, can account for the observation of all OI lines in He-O₂ collisions. The only atomic emissions observed for He-CO collisions are CI lines; He(³S) can supply sufficient energy to produce the upper states of these CI lines but not the OI lines as shown in Fig. 10. The NI lines from He-N₂ collisions are very weak and probably result from CIE or perhaps even energy pooling (internal and kinetic). Many of the OI and CI lines have been observed in thermal-energy studies of He*-CO¹⁷ and He*-O₂¹⁵ collisions, supporting the view that excitation transfer is the production mechanism. In both cases, the lines produced are those for which the upper states are nearly thermoneutral by dissociative excitation transfer.

As the H-atom kinetic energy is increased in H-N₂ collisions, N₂⁺(1N) emissions are observed with

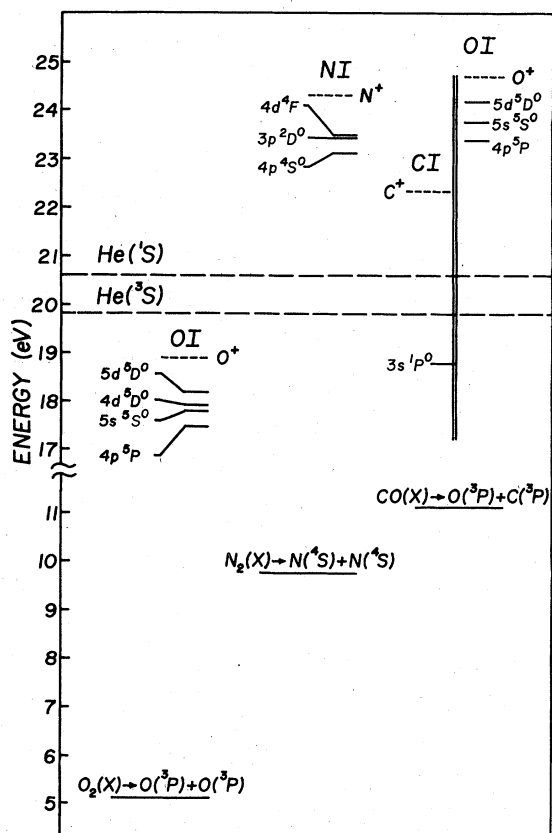


FIG. 10. Diagram showing the relations between the energy necessary to produce various atomic states from diatomic molecules and the metastable levels of He. Molecular parameters from Ref. 11.

increasing intensity. Production of N₂⁺(B), the upper state of the N₂⁺(1N) band system, probably results from the same type of CIE process that yields N₂(C) over the entire energy range. Table I shows the occupied molecular orbitals for the observed states of N₂, CO, O₂, and their ions. Promotion of a 2σ_u electron in N₂(X) yields N₂(C), while removal of a 2σ_u electron leads to ionization to N₂⁺(B). Thus production of N₂(C) and N₂⁺(B) may be viewed as resulting from the same type of collisional excitation. As noted earlier, N₂(B) is also produced in H-N₂ collisions; however, removal of a 3σ_g electron that must be promoted to obtain N₂(B) yields N₂⁺(X) which is not observable in our apparatus. The correlation between N₂(C) and N₂⁺(B) does, however, suggest that N₂⁺(X) is produced in substantial quantity. It is interesting that no N₂ or N₂⁺ states corresponding to promotion or removal of a 1π_u electron were observed in spite of the fact that several of these states are the upper states of known band systems which radiate in our detectable wavelength range. These states include the N₂⁺(A) state which we have ob-

TABLE I. Molecular orbital configurations of some diatomic molecular states. Only changes from the ground state of the neutral molecule are indicated.

State	Configuration	Energy (eV)
CO($X^1\Sigma^+$) ^a	KK(3 σ) ² (4 σ) ² (1 π) ⁴ (5 σ) ²	0
CO($a^1\Sigma^+$)	(1 π) ³ (2 π)	6.86
CO($d^3\Delta$)	(1 π) ³ (2 π)	7.52
CO($e^3\Sigma^-$)	(1 π) ³ (2 π)	7.89
CO($b^3\Sigma^+$)	(5 σ) ¹ (3s)	10.39
CO ⁺ ($X^2\Sigma^+$)	(5 σ) ¹	14.01
CO ⁺ ($A^2\Pi_u$)	(1 π) ³	16.54
CO ⁺ ($B^2\Sigma^+$)	(4 σ) ¹	19.67
N ₂ ($X^1\Sigma_g^+$) ^b	KK(2 σ_g) ² (2 σ_u) ² (1 π_u) ⁴ (3 σ_g) ²	0
N ₂ ($B^3\Pi_g$)	(3 σ_g) ¹ (1 π_g)	7.35
N ₂ ($C^3\Pi_u$)	(2 σ_u) ¹ (1 π_g)	11.03
N ₂ ⁺ ($X^2\Sigma_g^+$)	(3 σ_g) ¹	15.58
N ₂ ⁺ ($A^2\Pi_u$)	(1 π_u) ³	16.69
N ₂ ⁺ ($B^2\Sigma_g^+$)	(2 σ_u) ¹	18.75
O ₂ ($X^3\Sigma_g^-$) ^c	KK(2 σ_g) ² (2 σ_u) ² (3 σ_g) ² (1 π_u) ⁴ (1 π_g) ²	0
O ₂ ⁺ ($A^2\Pi_u$)	(1 π_u) ³	17.03
O ₂ ⁺ ($b^4\Sigma_g^-$)	(3 σ_g) ¹	18.17

^aReference 19.

^bF. R. Gilmore, J. Quant. Spectrosc. Radiat. Transfer **5**, 369 (1965).

^cReference 16.

served previously in charge-transfer studies.¹⁸

For CO, which is isoelectronic with N₂, the preferred ionic final state is CO⁺($A^2\Pi$), which results from removal of a 2 π electron from ground state CO. There are numerous neutral CO states that result from promotion of this electron (see Table I), and, as shown in Fig. 6, several of these states are observed. CO⁺($B-X$) first-negative (1N) emissions are not observed except at the highest kinetic energies. No known neutral CO states result from promotion of the 4 σ electron that must be removed to form CO⁺(B).¹⁹

While the H-N₂ and H-CO results are consistent in the sense that electrons which are promoted to yield neutral target emissions are relatively easily removed as the kinetic energy is increased, it is not clear why a π electron is preferred in CO but a σ electron in N₂. This situation is not peculiar to CIE by H-atom impact. Charge exchange collisions between a wide variety of positive ions and N₂ or CO generally yield predominately N₂⁺(B) or CO⁺(A), respectively.^{1,2} In fact, it seems generally true in ion-neutral collisions between 5–1000 eV and the neutral-neutral collisions reported here that the preferred product states, whether produced by CTE, CIE, or Penning ion-

ization, are those that are most active optically (in low-pressure discharges). Of course, for some systems it might be argued that this observation is a consequence of our experimental technique since optical emissions are detected, and from these data-product states and state distributions determined. However, there are a number of collision systems having more than one product excited state that radiate within our detectable wavelength range with lifetimes¹³ short enough to permit detection in our apparatus. Emissions from CO⁺(B) and CO⁺(A) are good examples as are emissions from N₂⁺(B) and N₂⁺(A). As noted above usually CO⁺(A) emissions ($\tau \sim 3$ μ sec) are stronger than those from CO⁺(B) ($\tau \sim 50$ nsec), while usually N₂⁺(B) emissions ($\tau \sim 50$ nsec), are stronger than those from N₂⁺(A) ($\tau \sim 10$ μ sec).

The results obtained with target oxygen molecules are consistent with this conclusion. For example, although the process



is less endothermic than



by about 1 eV, $b \rightarrow a$ first-negative emissions are considerably stronger than $A \rightarrow X$ second-negative emissions over the entire kinetic energy range. Similar results are obtained in He-O₂ collisions. Previous work on He⁺-O₂ charge-transfer collisions²⁰ yielded essentially no O₂⁺($c \rightarrow b$) Hopfield emissions in spite of the fact that production of O₂⁺(c) in such a collision is almost exactly thermo-neutral in these collisions. In this same work O₂⁺(1N) emissions again were much stronger than those from O₂⁺(2N). It has been implied, however, that predissociation of nascent O₂⁺(c) could preclude the observation of Hopfield emissions.²¹

The vibrational-state distribution of the cascade-free⁶ N₂(C) electronic state produced in H-N₂ and He-N₂ collisions remain essentially constant over the entire range of collision energies. These distributions are observed to be consistent with the predictions of a simple model based on vertical excitation and subsequent vertical decay, i.e., a Franck-Condon (FC) model. This is in agreement with the higher energy data of Birely⁶ for H-atom impact. Although unknown cascading prevents determination of N₂(B) state distributions, this state distribution is observed to remain constant over the entire range of collision energies. This suggests that all neutral N₂ excitations which occur in these collisions produce state distributions that are independent of kinetic energy. No determination of the CO-excited electronic-state vibrational distributions as a function of kinetic energy was made because of low photon yields at low ener-

gies. It is interesting, however, that in studies of neutral excitations by ion impact, Moore, using energy-loss spectra in H^+ , H_2^+ , and N^+ scattering from N_2 and CO at ~ 2 -3 keV, found agreement with the vertical transition model^{7,8} for different neutral excited states than those observed here. Earlier work in our laboratory⁹ showed that H^+ -NO(X) collisions yielded NO(A) vibrational-state distributions consistent with the vertical transition model; these distributions remained constant over the kinetic energy range 10-1000 eV.

The state distributions for $N_2^+(B)$ formed by H and He impact differ significantly especially at the lower energies. It is found that for H impact $v'=0$ and 1 are preferentially populated, while for He impact $v'=0-4$ are populated. According to the vertical transition model only $v'=0$ and 1 should be formed,²² and the ratio ($v'=1$):($v'=0$) should be 0.89:0.11. The experimentally observed ratio for 500-eV H- N_2 collisions is roughly 0.65:0.35. More quantitative information is difficult to obtain in the present experiments because of the low-photon flux. The important observations are that these deviations from FC behavior occur in neutral-neutral ionizing collisions and that the state distributions from these collisions approach the FC picture as the collision energy is increased. These observations further support the conclusion that distortion of the target molecule by the electric field of an incident ion is not the primary cause of non-FC behavior in ion-neutral CTE experiments.²³

It is apparent from these and other experiments that even at low velocities, neutral excitations in atom- (or ion-) neutral-molecule collisions proceed vertically at least for the systems studied. Ionizing collisions, whether CIE, CTE, or Penning ionization, generally proceed in a non-FC fashion. Without precise knowledge of the appropriate po-

tential-energy surfaces it is difficult to discuss these observations quantitatively. It is possible, within the framework of a curve-crossing model developed to describe such collisions, to make some general remarks. According to the model,²³ which assumes that vibrational excitation in the entrance channel is retained in the exit channels, when the upper and lower (adiabatic) potential energy surfaces cross at small atom- (ion-) molecule separation considerable vibrational excitation occurs, especially at low collision energies. For large separation at crossing and/or high kinetic energy there is little vibrational excitation, and the transitions proceed in a vertical fashion. Thus, based on the observed vertical nature of the neutral excitations at all kinetic energies, it may be inferred that these crossings occur where the coupling between relative motion and vibrational motion is weak.

As noted in Sec. III, the $O_2^+(b)$ vibrational-state distributions resulting from H- O_2 and He- O_2 impact, while different from each other, appear to remain constant as a function of kinetic energy. This conclusion is based on comparison of the relative heights of the peaks corresponding to the $\Delta v = 0, -1,$ and -2 sequences. Unfortunately, the individual bands comprising each sequence cannot be resolved so that small changes in each vibrational state distribution may not be detectable. It is apparent, however, that H- O_2 collisions produce $O_2^+(b)$ with a nearly FC distribution over the entire energy range; in contrast He produces a decidedly non-FC distribution.

ACKNOWLEDGMENT

This research was supported by the Department of Energy under Contract No. EY 76-S-02-2718.

¹See, for example, J. J. Leventhal, J. D. Earl, and H. H. Harris, *Phys. Rev. Lett.* **35**, 719 (1975); G. H. Bearman, J. D. Earl, R. J. Pieper, H. H. Harris, and J. J. Leventhal, *Phys. Rev. A* **13**, 1734 (1976), and references cited therein.

²D. Brandt, Ch. Ottinger, and J. Simonis, *Ber. Bunsenges. Phys. Chem.* **77**, 648 (1973).

³M. Lipeles, *J. Chem. Phys.* **51**, 1252 (1969).

⁴J. H. Moore, Jr., and J. P. Doering, *Phys. Rev.* **177**, 218 (1969).

⁵J. H. Birely, *Phys. Rev. A* **11**, 79 (1975).

⁶J. H. Birely, *Phys. Rev. A* **10**, 550 (1974).

⁷J. H. Moore, Jr., *Phys. Rev. A* **9**, 2043 (1974).

⁸J. H. Moore, Jr., and J. P. Doering, *J. Chem. Phys.* **52**, 1692 (1970).

⁹G. H. Bearman, J. D. Earl, H. H. Harris, P. B. James,

and J. J. Leventhal, *Chem. Phys. Lett.* **44**, 471 (1976).

¹⁰J. E. Bayfield, G. A. Khayrallah, and P. M. Koch, *Phys. Rev. A* **9**, 209 (1974).

¹¹B. Rosen, *Spectroscopic Data Relative to Diatomic Molecules* (Pergamon, Oxford, 1970).

¹²H. H. Harris and J. J. Leventhal, *J. Chem. Phys.* **64**, 3185 (1976).

¹³R. A. Anderson, *At. Data* **3**, 227 (1971).

¹⁴H. S. W. Massey and E. H. S. Burhop, *Electronic and Ionic Impact Phenomena* (Oxford University, London, 1952).

¹⁵W. C. Richardson and D. W. Setser, *J. Chem. Phys.* **58**, 1809 (1973).

¹⁶P. H. Krupenie, *J. Phys. Chem. Ref. Data* **1**, 423 (1972).

¹⁷W. B. Hurt and W. C. Grable, *J. Chem. Phys.* **57**, 734

(1972).

- ¹⁸H. H. Harris and J. J. Leventhal, *Electronic and Atomic Collisions, Abstracts of the Papers on the Ninth International Conference on the Physics of Electronic and Atomic Collisions*, edited by J. S. Risley and R. Geballe (University of Washington, Seattle, 1975), p. 991.
- ¹⁹P. H. Krupenie, *Natl. Stand. Ref. Data Ser.*, No. 5, (U.S. GPO, Washington, D.C., 1966).
- ²⁰H. H. Harris, M. G. Crowley, and J. J. Leventhal, *Chem. Phys. Lett.* 29, 540 (1974).
- ²¹R. F. Stebbings, A. C. H. Smith, and H. Ehrhardt, *J. Chem. Phys.* 39, 969 (1963).
- ²²D. A. Albritton, A. Schmeltekopf, and R. N. Zare, *Diatomic Intensity Factors* (Harper and Row, New York, to be published).
- ²³J. D. Kelley, G. H. Bearman, H. H. Harris, and J. J. Leventhal, *Chem. Phys. Lett.* 50, 295 (1977).